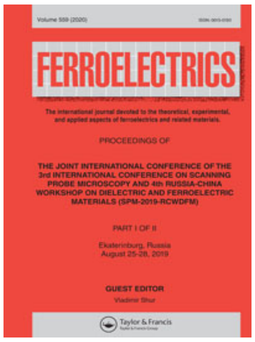

Ferroelectrics

ISSN: 0015-0193 (Print) 1563-5112 (Online) Journal homepage: https://www.tandfonline.com/loi/gfer20

Optical properties of the $HoGa_3(BO_3)_4$ crystal: experiment and *ab initio* calculation

S. N. Krylova, A. S. Aleksandrovsky, E. M. Roginskii, A. A. Krylov, I. A. Gudim & A. N. Vtyurin

To cite this article: S. N. Krylova, A. S. Aleksandrovsky, E. M. Roginskii, A. A. Krylov, I. A. Gudim & A. N. Vtyurin (2020) Optical properties of the $HoGa_3(BO_3)_4$ crystal: experiment and *ab initio* calculation, Ferroelectrics, 559:1, 135-140, DOI: 10.1080/00150193.2020.1722015

To link to this article: https://doi.org/10.1080/00150193.2020.1722015

Published online: 09 Jun 2020.

FERROELECTRICS
2020, VOL. 559, 135–140
https://doi.org/10.1080/00150193.2020.1722015

Taylor & Francis
Taylor & Francis Group

Optical properties of the $HoGa_3(BO_3)_4$ crystal: experiment and *ab initio* calculation

S. N. Krylova[a], A. S. Aleksandrovsky[a,b], E. M. Roginskii[c,d], A. A. Krylov[e], I. A. Gudim[a], and A. N. Vtyurin[a,b]

[a]Kirensky Institute of Physics Federal Research Center KSC SB RAS, Krasnoyarsk, Russia; [b]Siberian Federal University, Krasnoyarsk, Russia; [c]Ioffe Institute, St. Petersburg, Russia; [d]St. Petersburg State University, St. Petersburg, Russia; [e]Moscow Institute of Physics and Technology, Dolgoprudny, Russia

ABSTRACT
Single crystal of $HoGa_3(BO_3)_4$ has been grown using solution-melt synthesis. The optical band gap determined from the measured absorption spectrum is due to direct allowed transition and equals to 4.14 eV. The optical properties of this crystal are calculated by the plane-wave pseudo-potential method based on density functional theory. The structure of the crystal has been optimized. The electronic structure of $HoGa_3(BO_3)_4$ is calculated. The experimental and theoretical fundamental absorption spectra are compared. The calculated bandgap is in good agreement with the experimental data.

ARTICLE HISTORY
Received 28 August 2019
Accepted 25 November 2019

KEYWORDS
$HoGa_3(BO_3)_4$; *ab initio* calculation; absorption spectrum; band structure

1. Introduction

The crystals with huntite structure attract considerable attention due to their exciting magnetic and magnetoelectric properties. A number of studies on $RM_3(BO_3)_4$ crystals (R = Ho, Nd, Y, Pr, Yb, Sm, Eu, Gd, Tb, Dy, Tm) is devoted to aluminum borates [1–3]. The studies of the rare earth iron borates properties are wide presented [4–9]. $HoGa_3(BO_3)_4$ crystal belongs to the same space group R32 as aluminum borates and has been studied much less. The interesting work is devoted to high-temperature crystallization, structure and X-ray diffraction of rare earth gallium borates [10]. This article includes experimental information about crystal growth, IR spectra, luminescence and excitation spectra, and micro-hardness of gallium borates. At the same time, as was found, $HoGa_3(BO_3)_4$ shows an unusually large magnetoelectric effect [11]. Thus, holmium gallium borate is to be considered as a promising material not only for luminescent [10] and nonlinear laser applications, but also for the use in spintronic devices. The optical properties of this crystal are not studied.

The study of the optical properties of $HoGa_3(BO_3)_4$ is of interest not only from a cognitive point of view, but also in terms of practical application in the field of laser and nonlinear optics and spintronics. This work aims at the experimental and theoretical investigation of the optical properties of $HoGa_3(BO_3)_4$ crystal.

CONTACT S. N. Krylova slanky@iph.krasn.ru.

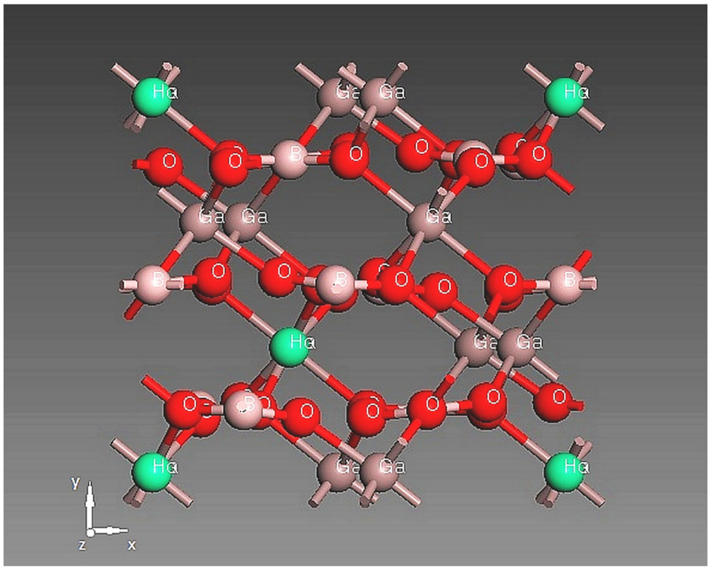

Figure 1. The $HoGa_3(BO_3)$ crystal structure in the *R*32 phase.

2. Experiment and calculation

Single crystals of the $HoGa_3(BO_3)_4$ have been grown using solution-melt synthesis [12]. The samples were optically transparent yellow plates cut from a single crystal with a size of about $4 \times 3 \times 1.5\,mm^3$ and did not contain any inclusions being visible under a microscope. Absorption spectra were recorded using Shimadzu UV-3600 spectrometer equipped with a double monochromator.

The theoretical calculations were carried out by the plane-wave pseudo-potential method based on DFT using Cambridge Serial Total Energy Package code (CASTEP) [13]. Pseudo-atom calculations are performed for B: 2s2, 2p1; O: 2s2, 2p4; Ga: 3d10,4s2, 4p1; and Ho: 4f11, 5s2, 5p6, 6s2. We used the generalized gradient approximation (GGA) with the Perdew-Burke-Ernzerhof (PBE) functional [14], which was proven to provide good results for solids of high density [15]. The structures were relaxed using the Broyden, Fletcher, Goldfarb, and Shannon (BFGS) minimization method algorithm [16]. The lattice constants and atom coordinates were optimized by minimizing the total energy. Through a series of convergence studies concerning cutoff energies and k-points, the cutoff energies were set to 900 eV, and the K-space integration over the Brillouin zone was carried out using a $3 \times 3 \times 3$ k-point Monkhorst-Pack mesh. All these parameters were tested to ensure that the self-consistent total energies converged to within $1.0 \cdot 10^{-7}$ eV/atom.

3. Results and discussion

$HoGa_3(BO_3)_4$ belongs to a trigonal symmetry class (the space symmetry group *R*32 (No. 155)). The crystal structure is presented in Figure 1. Wyckoff positions of Ho, B, Ga, and O are 3a, 3b, 9d, 18f, and 9e, correspondingly [17–19]. The main structural elements of $HoGa_3(BO_3)_4$ are GaO_6 octahedra, BO_3 triangles, and HoO_6 triangular prisms.

Table 1. Lattice parameters in the R32 phase of the compounds $HoR_3(BO_3)_4$ (R = Ga, Fe).

	$HoGa_3(BO_3)_4$	$HoFe_3(BO_3)_4$
A_{exp} (A)	5.99 [18]	6.046 [19]
α_{exp}	104.07 [18]	103.089 [19]
A_{calc} (A)	6.063 [this work]	6.097 [20]
α_{calc}	104.08 [this work]	103.90 [20]

The BO_3 groups are arranged in layers, and the Ga atoms are arranged in helicoidal chains.

The geometry optimization allows refining the geometry of a 3D periodic system to obtain a stable structure. This is done by performing an iterative process, in which the coordinates of the atoms and the cell parameters are adjusted so that the total energy of the structure is minimized. The geometry optimization is based on reducing the magnitude of calculated forces and stresses until they become smaller than defined convergence tolerances. The process of geometry optimization generally results in a model structure that closely resembles the real structure. To obtain a stable geometry structure, we have made the structural relaxation and optimization with the approximations (LDA), to determine the internal atomic coordinates and structure parameters.

The obtained lattice parameters are listed in Table 1, together with the available experimental results [18] and $HoFe_3(BO_3)_4$ [19, 20] data for comparison. From Table 1, it could be seen that the obtained equilibrium lattice constants are in good agreement with experimental data for both crystals and the theoretical values for the isostructural crystal.

Figure 2 presents the fragment of the band structure of $HoGa_3(BO_3)_4$ that includes its valence and conduction bands. The top of the valence band is mainly formed by O 2p, B 2s, and B 2p orbitals. The bottom of the conduction band is formed by Ho 5d and B 2p orbitals. In certain difference to $YAl_3(BO_3)_4$, where indirect bandgap is slightly narrower than direct ones [21], in $HoGa_3(BO_3)_4$ the direct bandgap is the narrowest, and according to the calculation it equals to 4.17 eV at Γ point. This direct bandgap corresponds to the transition from O 2p orbital to Ho 5d one. Therefore, the direct allowed transition must primarily contribute to the formation of the fundamental absorption edge.

The unpolarized absorption spectrum of $HoGa_3(BO_3)_4$ in the vicinity of the fundamental absorption edge, is presented in Figure 3 (red line). The region from 3 to 3.8 eV contains ff transitions of Ho^{3+} ion.

The analysis of the experimental absorption spectrum of $HoGa_3(BO_3)_4$ is performed using Tauc's approach version recently used in Ref. [22]:

$$\alpha\ h\nu = \beta(h\nu\ - E_g)^n, \tag{1}$$

where β is the inverse of the band edge parameter, $h\nu$ is the photon energy, and E_g is the bandgap. The fitting does not allow distinguishing between different types of transitions; therefore, from the band structure calculations, n was taken to be ½. The result of the fitting is shown in Figure 3 by the blue line and gives E_g = 4.14 eV, which demonstrates a good agreement with calculated value of 4.17 eV. It is interesting to note

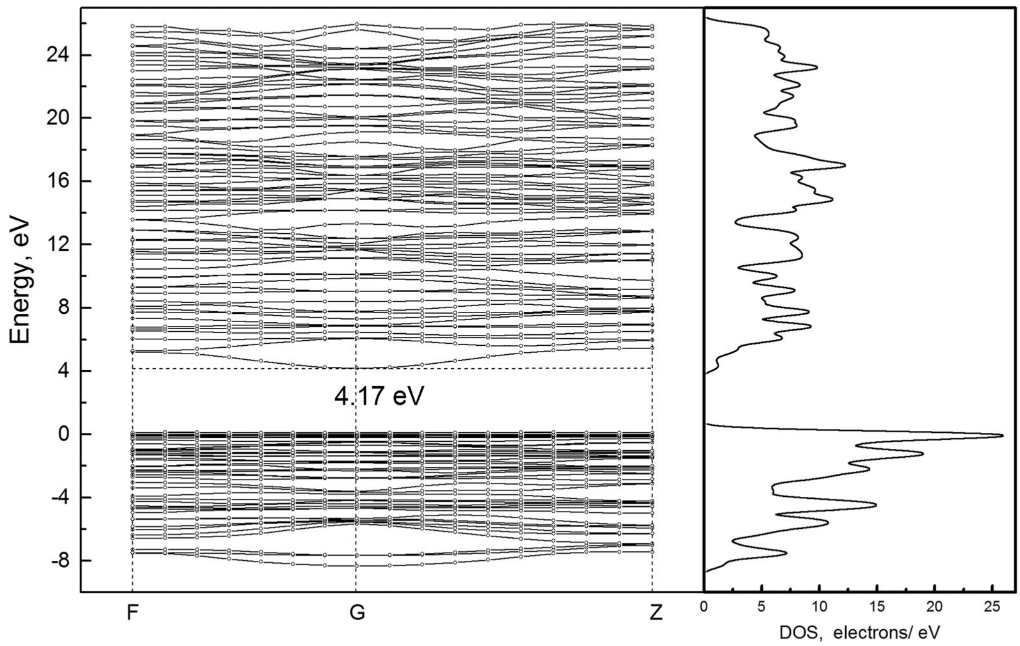

Figure 2. The fragment of the calculated electronic band structure of the $HoGa_3(BO_3)_4$ crystal.

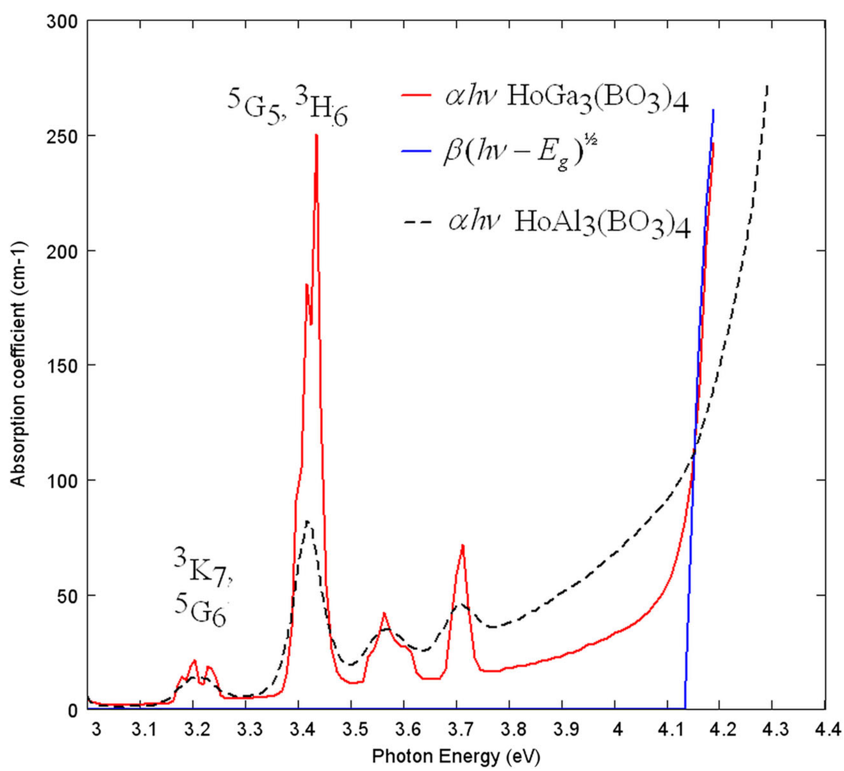

Figure 3. The fundamental absorption edge: absorption dependence on photon energy.

that for holmium aluminum borate with the huntite structure a narrower bandgap is expected (for comparison, the spectrum is presented in Figure 3 by the dashed line).

4. Conclusion

The absorption spectrum of $HoGa_3(BO_3)^+$ in the visible/UV spectral range, contains a contribution from f-f transitions of Ho^{3+} ion and that from interband transitions. The fundamental absorption edge is formed mainly by direct allowed transitions. The band structure of $HoGa_3(BO_3)_4$ is calculated by the plane-wave pseudo-potential method based on DFT. The calculated bandgap 4.17 eV is in a good agreement with that determined from the absorption spectrum (4.14 eV).

Funding

This work was supported by the Russian Foundation for Basic Research (grant No 18-02-00754).

References

[1] K. C. Liang *et al.*, Giant magnetoelectric effect in $HoAl_3(BO_3)_4$, *Phys. Rev. B* **83** (18), 180417 (2011). DOI: 10.1103/PhysRevB.83.180417.
[2] H. Y. P. Hong and K. Dwight, Crystal structure and fluorescence lifetime of $NdAl_3(BO_3)_4$ a promising laser material, *Mater. Res. Bull.* **9** (12), 1661 (1974). DOI: 10.1016/0025-5408(74)90158-5.
[3] E. A. Dobretsova *et al.*, IR spectroscopy of rare-earth aluminum borates $RAl_3(BO_3)_4$ (R = Y, Pr–Yb), *Opt. Spectrosc.* **116** (1), 77 (2014). DOI: 10.1134/S0030400X14010068.
[4] A. S. Krylov *et al.*, Manifestation of magnetoelastic interactions in Raman spectra of $Ho_xNd_{1-x}Fe_3(BO_3)_4$ crystals, *J. Adv. Dielect.* **08** (02), 1850011 (2018). DOI: 10.1142/S2010135X1850011X.
[5] A. Krylov *et al.*, Low-temperature features of Raman spectra below magnetic transitions in multiferroic $Ho_{1-x}Nd_xFe_3(BO_3)_4$ and $Sm_{1-y}La_yFe_3(BO_3)_4$ single crystals, *Ferroelectrics* **510**, 92 (2017). DOI: 10.1080/00150193.2017.1294040.
[6] A. S. Krylov *et al.*, Magnetoelastic interactions in Raman spectra of $Ho_{1-x}Nd_xFe_3(BO_3)_4$ crystals, *Solid State Commun.* **174**, 26 (2013). DOI: 10.1016/j.ssc.2013.09.011.
[7] A. S. Krylov *et al.*, Raman study of $HoFe_3(BO_3)_4$ at simultaneously high pressure and high temperature: p-T phase diagram, *J. Raman Spectrosc.* **48** (11), 1406 (2017). DOI: 10.1002/jrs.5078.
[8] E. Moshkina *et al.*, Temperature-dependent absorption lines observation in Raman spectra of $SmFe_3(BO_3)_4$ ferroborate, *J. Raman Spectrosc.* **49** (10), 1732 (2018). DOI: 10.1002/jrs.5430.
[9] E. Moshkina *et al.*, Crystal growth and Raman spectroscopy study of $Sm_{1-x}La_xFe_3(BO_3)_4$ ferroborates, *Cryst. Growth Des.* **16** (12), 6915 (2016). DOI: 10.1021/acs.cgd.6b01079.
[10] L. I. Al'shinskaya, N. I. Leonyuk, and T. I. Timchenko, High-temperature crystallization, composition, structure, and certain properties of rare-earth gallium borates, *Krist. Technol.* **14**, 897 (1979). DOI: 10.1002/crat.19790140802.
[11] N. V. Volkov *et al.*, Magnetization, magnetoelectric polarization, and specific heat of $HoGa_3(BO_3)_4$, *JETP Lett.* **99** (2), 67 (2014). DOI: 10.1134/S0021364014020106.
[12] L. N. Bezmaternykh *et al.*, Crystallization of trigonal (Tb,Er)(Fe,Ga)$_3(BO_3)_4$ phases with hantite structure in bismuth trimolybdate-based fluxes, *Crystallogr. Rep.* **50** (S1), S97 (2005). DOI: 10.1134/1.2133981.

[13] S. J. Clark *et al.*, First principles methods using CASTEP, Z. *Kristallogr. Cryst. Mater*. **220**, 567 (2005).
[14] J. P. Perdew, K. Burke, and M. Ernzerhof, Generalized gradient approximation made simple, *Phys. Rev. Lett*. **77** (18), 3865 (1996). DOI: 10.1103/PhysRevLett.77.3865.
[15] L. Szeleszczuk, D. M. Pisklak, and M. Zielińska-Pisklak, Can we predict the structure and stability of molecular crystals under increased pressure? First-principles study of glycine phase transitions, *J. Comput. Chem*. **39** (19), 1300 (2018). DOI: 10.1002/jcc.25198.
[16] B. G. Pfrommer *et al.*, Relaxation of crystals with the quasi-Newton method, *J. Comp. Physiol*. **131** (1), 233 (1997). DOI: 10.1006/jcph.1996.5612.
[17] S. A. Klimin *et al.*, Evidence for differentiation in the iron-helicoidal chain in $GdFe_3(BO_3)_4$, *Acta Crystallogr. B Struct. Sci.* **61** (5), 481 (2005). DOI: 10.1107/S0108768105017362.
[18] E. Yu. Borovikova *et al.*, Crystal growth, structure, infrared spectroscopy, and luminescent properties of rare-earth gallium borates $RGa_3(BO_3)_4$, R = Nd, Sm-Er, Y, *Opt. Mater*. **49**, 304 (2015). DOI: 10.1016/j.optmat.2015.09.021.
[19] Y. Hinatsu *et al.*, Magnetic and calorimetric studies on rare-earth iron borates $LnFe_3(BO_3)_4$ (Ln = Y, La-Nd, Sm-Ho), *J. Solid State Chem*. **172** (2), 438 (2003). DOI: 10.1016/S0022-4596(03)00028-8.
[20] M. S. Pavlovskiy, V. I. Zinenko, and A. S. Shinkorenko, Effect of a rare-earth ion on the structural instability in $RFe_3(BO_3)_4$ crystals, *JETP Lett*. **108** (2), 116 (2018). DOI: 10.1134/S0021364018140114.
[21] Y. Wang, L. Wang, and H. Li, Electronic structure and linear optical properties of $YAl_3(BO_3)_4$, *J. Appl. Phys*. **102** (1), 013711 (2007). DOI: 10.1063/1.2752109.
[22] D. M. Guzman and A. Strachan, Structural and electronic properties of copper-doped chalcogenide glasses, *Phys. Rev. Mater*. **1**, 055801 (2017).